Renormalization persistency of the tensor force in nuclei

Naofumi Tsunoda
Department of Physics, University of Tokyo, 7-3-1 Hongo, Bunkyo-ku, Tokyo, Japan

Takaharu Otsuka
Department of Physics and Center for Nuclear Study, University of Tokyo, 7-3-1 Hongo, Bunkyo-ku, Tokyo, Japan and National Superconducting Cyclotron Laboratory, Michigan State University, East Lansing, Michigan 48824, USA

Koshiroh Tsukiyama
Department of Physics and Center for Nuclear Study, University of Tokyo, 7-3-1 Hongo, Bunkyo-ku, Tokyo, Japan

Morten Hjorth-Jensen
Department of Physics and Center of Mathematics for Applications, University of Oslo, N-0316 Oslo, Norway and National Superconducting Cyclotron Laboratory, Michigan State University, East Lansing, Michigan 48824, USA

(Received 18 August 2011; published 24 October 2011)

In this work we analyze the tensor-force component of effective interactions appropriate for nuclear shell-model studies, with particular emphasis on the monopole term of the interactions. Standard nucleon-nucleon (NN) interactions such as AV8' and χN^{3}LO are tailored to shell-model studies by employing $V_{\mathrm{low}k}$ techniques to handle the short-range repulsion of the NN interactions and by applying many-body perturbation theory to incorporate in-medium effects. We show, via numerical studies of effective interactions for the sd and the pf shells, that the tensor-force contribution to the monopole term of the effective interaction is barely changed by these renormalization procedures, resulting in almost the same monopole term as the one of the bare NN interactions. We propose to call this feature *renormalization persistency* of the tensor force, as it is a remarkable property of the renormalization and should have many interesting consequences in nuclear systems. For higher multipole terms, this feature is maintained to a somewhat smaller extent. We present general intuitive explanations for the renormalization persistency of the tensor force as well as analyses of core-polarization terms in perturbation theory. The central force does not exhibit a similar renormalization persistency.

DOI: 10.1103/PhysRevC.84.044322 PACS number(s): 21.30.Fe, 21.60.Cs

I. INTRODUCTION

The nucleon-nucleon (NN) interaction is normally modeled in terms of several components, such as a central force, a spin-orbit force, and a tensor force. These mathematical terms accommodate our phenomenological knowledge of the strong interaction, which, when used in a nuclear many-body context, is subjected to different renormalization procedures. For the nuclear many-body problem, a given renormalization procedure leads to the derivation of an effective interaction, starting from a bare realistic NN interaction. The so-called bare NN interactions exhibit a strong coupling between low-momentum and high-momentum degrees of freedom generated from short-range details of the interaction. By "bare" we mean that the above-mentioned strong coupling is left untouched. This coupling is included only implicitly, via various renormalization procedures, in the effective interactions used in, for example, shell-model studies.

As an example of bare NN interactions, the Argonne interactions (AV), which are defined in terms of local operators in coordinate space, show a strong short-range repulsion [1,2]. The resulting strong coupling between low- and high-momentum modes makes the many-body problem highly nonperturbative. On the other hand, in shell-model calculations, the employed effective interactions are defined for a specific configuration space (a strongly reduced Hilbert space), normally called the model space. Therefore, the effective interactions for the shell model should be renormalized to include the effects of virtual excitations to the configurations not included in the model space.

Although the properties and the effects of the full interaction and various renormalized interactions have been investigated extensively over the years, we feel that there are still important features of the nuclear interaction that deserve some special attention. In particular, we show here via several numerical studies that the tensor-force component of the bare nuclear interaction is left almost unaffected by various renormalization procedures. The monopole component of the tensor force, a component of great interest in studies of shell evolution (see discussion below) in nuclei toward the drip lines, is left almost unchanged under various renormalizations. This allows us thereby to extract simple physics interpretations from complicated many-body systems. In this work we label such a lack of renormalization influence as *renormalization persistency* (RP). The RP is a property exhibited by specific terms of the original nuclear Hamiltonian that are not affected, or barely affected, by the renormalization procedure.

On the experimental side, present and future radioactive ion-beam facilities have made it possible to perform experiments that explore nuclei far from the stability line of the nuclear chart. Many unexpected and new phenomena have been observed in such experiments carried out at radioactive

ion-beam facilities worldwide. One of the most striking results is the breaking of the conventional shell structures in neutron-rich nuclei. Such shell evolution, unexpected in the past, is known by now to occur mainly due to an unbalanced neutron to proton ratio and specific orbital-dependent components of the nuclear forces. In particular, the nuclear tensor force plays a key role here, as proposed by one of the authors [3,4]. One of the most useful quantities to probe the effect of tensor force is the so-called monopole matrix element. The monopole matrix element [5,6] of the two-body interaction between two single-particle states labeled j and j' and total two-particle isospin T is defined as

$$V^T_{j,j'} = \frac{\sum_J (2J+1)\langle jj'|V|jj'\rangle_{JT}}{\sum_J (2J+1)} \tag{1}$$

for $j \neq j'$.[1] Here $\langle \cdot\cdot|V|\cdot\cdot\rangle_{JT}$ denotes the antisymmetrized two-body matrix element coupled to total angular momentum J and total isospin T. The monopole matrix element is crucial for shell evolution because it affects the effective single-particle energy linearly. For instance, if $n_n(j')$ neutrons occupy the single-particle state j', they shift the effective single-particle energy of protons in the state j as follows:

$$\Delta\epsilon_p(j) = \tfrac{1}{2}\left(V^{T=0}_{jj'} + V^{T=1}_{jj'}\right) n_n(j'), \tag{2}$$

where $\Delta\epsilon_p(j)$ represents the change of the effective single-particle energy of protons in the single-particle state j. When we consider the tensor-force contribution, the monopole matrix elements always have different signs between a pair of spin-orbit partners. For example, the interaction matrix elements $V_{j_> j'}$ and $V_{j_< j'}$ have opposite signs. Here we define $j_>$ and $j_<$ to represent the spin-orbit partners, that is, $j_> = l + 1/2$ and $j_< = l - 1/2$, where l stands for the orbital momentum of a given single-particle state. In this case, the tensor-force changes the spin-orbit splitting between $j_>$ and $j_<$. The shell structure is also altered, particularly if we have a sizable number of neutrons in the single-particle state j'.

In previous studies [3], the tensor-force component in effective interactions for shell-model calculations was, for the sake of simplicity, modeled via the exchange of π and ρ mesons only. To a large extent, this yields results close to the tensor force in realistic NN interactions. In fact, this model describes rather well the experimental data in several mass regions [4]. However, it is far from trivial that the tensor force in effective interactions for the shell model can be considered to be given by the exchange of π and ρ mesons only.

The aim of this article is thus to investigate the RP of the nuclear tensor force and to understand the validity of the above assumption through theoretical studies, based on realistic NN interactions and microscopic theories for deriving effective interactions, focusing on the effective interaction for the shell model.[2]

[1] For the $j = j'$ case, the definition is slightly different.

[2] A short version of the present results was included in Ref. [4], while more substantial, deeper, and wider discussions are given in this paper.

This work is organized as follows. First, we briefly review the theory for constructing effective interactions in Sec. II. In Secs. III, IV and V, the RP of the monopole part of the tensor force from various approaches to the effective interactions will be discussed. In Sec. VI we present not only the monopole part but also the two-body matrix elements including the multipole part of the various effective interactions and discuss their tensor force components. For the sake of completeness, we include analyses using other NN interactions in Sec. VII. The last section contains our conclusions.

II. CONSTRUCTION OF THE EFFECTIVE INTERACTION FOR THE SHELL MODEL

The aim of this section is to give a brief sketch of the theoretical methods we employ in our analyses of the nuclear force. To construct the effective interactions for the nuclear shell model, we use many-body perturbation theory (MBPT). However, as inputs to MBPT, we cannot use bare realistic NN interactions directly since their high-momentum components make MBPT nonconvergent [7]. We integrate out these high-momentum components employing a renormalized interaction defined only in the low-momentum space below a certain sharp cutoff Λ and designed not to change two-body observables like NN scattering data [8]. This recipe defines a cutoff-dependent family of interactions, normally labeled as $V_{\mathrm{low}k}(\Lambda)$, which, to be more specific, can be written as

$$V_{\mathrm{low}k}(\Lambda) = P_\Lambda V_{\mathrm{bare}} P_\Lambda + \delta V_{ct}(\Lambda), \tag{3}$$

where P_Λ indicates a projection operator onto the low-momentum space below Λ. The term $\delta V_{ct}(\Lambda)$ represents the correction term coming from the renormalization procedure. In other words, $P_\Lambda V_{\mathrm{bare}} P_\Lambda$ is a simple projection to a low-momentum space, while $\delta V_{ct}(\Lambda)$ emerges as a result of the chosen renormalization procedure. By construction, $V_{\mathrm{low}k}(\Lambda)$ approaches the original NN interaction in the limit $\Lambda \to \infty$. A complete renormalization scheme would generate higher-body forces as well, such as three-body and four-body forces, $V_{3\mathrm{N}}$ and $V_{4\mathrm{N}}$, respectively. In this work we limit ourselves to two-body ($V_{2\mathrm{N}}$) interactions only. Thus the cutoff dependence of physical quantities can be used to assess the error made by omitting more complicated many-body forces. The term $P_\Lambda V_{\mathrm{bare}} P_\Lambda$ should contain the long-range part of one-pion exchange interaction as a major component.

Next, we proceed to MBPT. The low-momentum interaction $V_{\mathrm{low}k}$ is a good starting point for MBPT because we can avoid the difficulty caused by the strong short-range repulsion. For a degenerate model space, the effective interaction V_{eff} can be written as

$$V_{\mathrm{eff}} = \hat{Q} - \hat{Q}' \int \hat{Q} + \hat{Q}' \int \hat{Q} \int \hat{Q} - \cdots, \tag{4}$$

where $\hat{Q}(E_0)$ is the so-called $\hat{Q}$ box, defined as

$$\hat{Q}(E_0) \equiv PH_1P + PH_1Q\frac{1}{E_0 - QHQ}QH_1P. \tag{5}$$

Here the Hamiltonian is divided into an unperturbed part H_0 and an interaction part H_1, $H = H_0 + H_1$, and the model

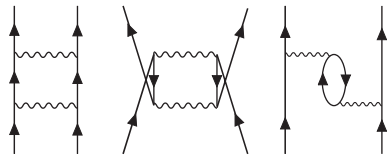

FIG. 1. Examples of diagrams to second order in the interaction H_1 included in the $\hat{Q}$ box. The diagrams are referred to as (a) particle-particle ladder, (b) hole-hole ladder, and (c) core polarization, respectively.

space is set to be degenerate with respect to the unperturbed Hamiltonian H_0 with energy E_0. The integration symbols in Eq. (4) represent the inclusion to infinite order of so-called folded diagrams; see Refs. [9,10] for details. The $\hat{Q}$ box is given by diagrams that are valence linked and irreducible, while $\hat{Q}'$ indicates that only diagrams that are of second or higher order in terms of the interaction H_1 are included; see, for example, Fig. 1.

We can solve Eq. (4) by the following iterative formula:

$$V_{\rm eff}^{(n)} = \hat{Q}(E_0) + \sum_{m=1}^{\infty} \hat{Q}_m(E_0)\left\{V_{\rm eff}^{(n-1)}\right\}^m, \tag{6}$$

where $\hat{Q}_m(E_0) = \frac{1}{m!}(\frac{d^m \hat{Q}(\omega)}{d\omega^m})_{\omega=E_0}$. In this work, we take into account diagrams up to second or third order in the interaction H_1 for the calculation of the $\hat{Q}$ box.

By using this two-step method, we can start from an arbitrary bare realistic NN interaction. We calculate effective interactions starting from AV8' [1,2] and the chiral χN^{3}LO interaction [11]. Results using the AV8' interaction are shown in the following sections, while our results obtained with the χN^{3}LO interaction are shown in Sec. VII for the sake of completeness.

Finally, to extract the tensor component from the obtained effective interactions, we employ the spin-tensor decomposition employed in, for example, Refs. [12–14]:

$$\begin{aligned}&\langle abLS|V_p|cdL'S'\rangle_{J'T}\\ &= (-1)^{J'}\hat{p}\begin{Bmatrix} L & S & J' \\ S' & L' & p \end{Bmatrix}\sum_J (-1)^J \hat{J}\begin{Bmatrix} L & S & J \\ S' & L' & p \end{Bmatrix}\\ &\quad\times\langle abLS|V|cdL'S'\rangle_{JT},\end{aligned} \tag{7}$$

where $\langle\cdots LS|V|\cdots L'S'\rangle_{JT}$ denotes the LS-coupled matrix element of the effective interaction. Here a (as well as bcd) is shorthand for the set of quantum numbers (n_a, l_a) and so on. The operator V_p is defined as the scalar product $V_p \equiv U^{(p)}\cdot X^{(p)}$, where $U^{(p)}$ and $X^{(p)}$ are irreducible tensors of rank p, applying to operators in both spin and coordinate space. The tensor component is extracted by setting $p = 2$ in Eq. (7). Finally, in the above equation we have defined $\hat{p} = 2p + 1$ and $\hat{J} = 2J + 1$.

III. TENSOR FORCE IN LOW-MOMENTUM INTERACTION $V_{\rm low}k$

We now present results obtained by the theoretical methods described in the previous section. Figure 2 shows the monopole part of the tensor-force of the renormalized $V_{\rm low}k$ interaction derived from the Argonne V8' (AV8') potential for the sd shell and the pf shell. The cutoff value Λ varies from 1.0 to 5.0 fm^{-1}. Here we employ units where $c = \hbar = \hbar^2/m = 1$.

The typical value of the cutoff is determined by the best reproduction of the binding energies of ^{3}H and ^{4}He. The resulting cutoff value lies around 2.0 fm^{-1} [15]. A too small cutoff Λ (for example, 1.0 fm^{-1} in momentum space) cannot resolve the necessary degrees of freedom. Since the Compton length of the pion is approximately 0.7 fm, a cutoff $\Lambda = 1.0$ fm^{-1}, which corresponds to 1.0 fm in coordinate space, is too small to resolve the exchange of a pion. Although the resulting renormalized interaction $V_{\rm low}k$ with $\lambda = 1.0$ fm^{-1} may not contain an appropriate tensor force for shell-model calculations, we include its result in Fig. 2 and subsequent similar figures for the sake of completeness.

We now present the results for the cutoff values $\Lambda = 1.0, 2.1$, and 5.0 fm^{-1} in Fig. 2. The matrix elements are calculated using a harmonic oscillator basis with $\hbar\omega = 14$ and 11 MeV for the sd shell and the pf shell, respectively. Except for a very low (and thereby unreasonable) cutoff value $\Lambda = 1.0$ fm^{-1}, one finds, both in the sd shell and the pf shell, that the monopole part of the tensor force of $V_{\rm low}k$ has almost no cutoff dependence and has almost the same strength as that of the original NN interaction. Thus, within the usual values of the cutoff, we can see that the monopole part of the tensor force fulfills the RP almost perfectly with respect to the renormalization of the short-range part of the NN interaction.

We look now into the robustness and the generality of the features discussed above. For this purpose, we consider the relative motion of two interacting nucleons. The orbital angular momentum of the relative motion can be $L = 0$ (S), 1 (P), 2 (D), etc. If the tensor force is acting between two states, there is no coupling between two S states because the relative coordinate operator in the tensor force is of rank 2. The S-to-S coupling is thus zero. This results in strongly suppressed contributions to the tensor force from the short-range part of the relative-motion wave function since a good fraction of the short-range repulsion stems from S waves. Partial waves higher than S waves carry also a centrifugal barrier component that results in a smaller short-range contribution to the tensor force relative to S waves. Thus, changes of the potential at short distances do not affect matrix elements of the tensor force for low momentum states. This seems to be the basic reason why the tensor force remains almost the same throughout the renormalization procedure. In other words, there is a sound reason to expect the RP for the tensor force regarding the treatment of the short-range correlation. On the other hand, the present argument may not be applied to other parts of the nuclear force such as the central force.

The second term δV of Eq. (3) is due to the renormalization. It includes, for example, the central-force component at intermediate internucleon distances and may affect, in principle, the tensor force as well. The first term, $P_\Lambda V_{\rm bare} P_\Lambda$, is equal to

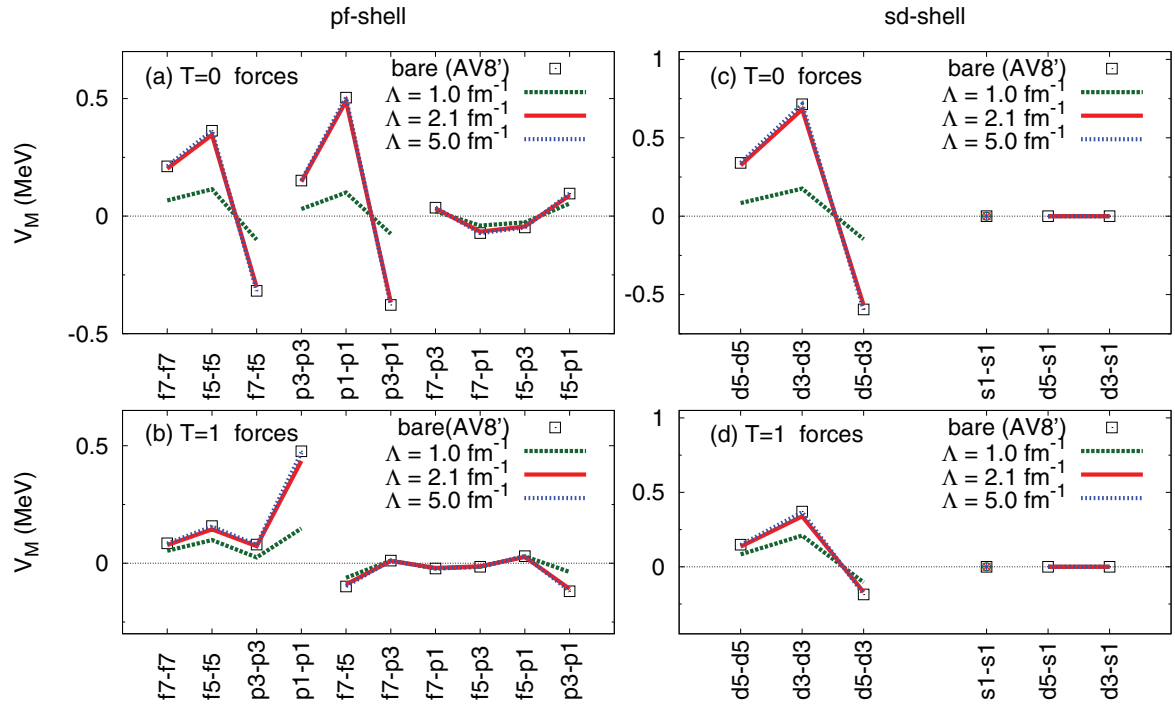

FIG. 2. (Color online) Tensor-force monopole component of low-momentum interaction $V_{\mathrm{low}k}$ as function of the cutoff parameter Λ for (a) $T = 0$ forces in the pf shell, (b) $T = 1$ forces in the pf shell, (c) $T = 0$ forces in the sd shell, and (d) $T = 1$ forces in the sd shell. The cutoff parameter Λ of $V_{\mathrm{low}k}$ varies from 1.0 to 5.0 fm^{-1}.

the bare tensor force in the limit of $\Lambda \to \infty$ by definition. In this limit δV is zero. Since matrix elements of the tensor force, particularly for low-momentum states, are not affected much by the short-range modification, the effect of the tensor-force component in the first term of Eq. (3) remains the same to a large extent, even with finite Λ values, unless it becomes extremely small. The fact that the RP is almost fulfilled in numerical calculations (as we can see in Fig. 2) implies therefore that the second term δV results in small contributions to the tensor force or does not change the long-range part of the tensor force. The origin of the weak tensor-force component in δV can be understood by the arguments presented in Sec. V, arguments that are based on the close relation between the $V_{\mathrm{low}k}$ renormalization process and contributions from MBPT that represent long-range corrections, as discussed in Refs. [8,16] as well. We shall come back to this point in Sec. V.

IV. RENORMALIZATION OF THE CENTRAL FORCE

Contrary to the tensor force, it can be seen from our numerical studies that the central force does not fulfill the RP and is, indeed, affected strongly by the renormalization procedure due to the short-range part of the NN interaction. This is reflected in a much stronger cutoff dependence as well. The central-force monopole part of δV in Eq. (3) is thus not small.

Figure 3 shows the monopole part of the central force of the bare AV8' potential obtained by the decomposition of Eq. (7). In Fig. 3 we show also the corresponding central-force monopole component using the $V_{\mathrm{low}k}$ renormalized interaction originating from the AV8' potential, labeled full. We show also results where the tensor-force component has been subtracted from the bare NN interaction in the renormalization procedure, labeled TS in Fig. 3. What we can see in Fig. 3 is the effect of the renormalization due to the short-range part of the bare realistic NN interaction. The difference between bare AV8' and $V_{\mathrm{low}k}$ (TS) lies mainly in the renormalization due to the short-range part of the central force, as the tensor force is subtracted in $V_{\mathrm{low}k}$ (TS). On the other hand, the difference between $V_{\mathrm{low}k}$ (TS) and $V_{\mathrm{low}k}$ (full) comes solely from the renormalization due to the short-range part of the tensor force.

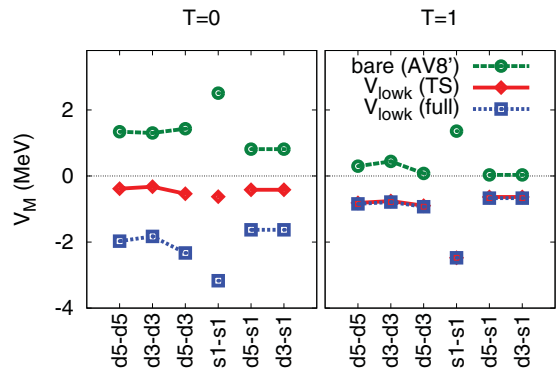

FIG. 3. (Color online) Central-force component of the monopole term of the bare AV8', $V_{\mathrm{low}k}$ (TS), and $V_{\mathrm{low}k}$ (full) for the sd shell; see text for further details and discussion. The central-force component is obtained using the decomposition of Eq. (7). The effect of the renormalization on the short-range tensor force is also shown. The cutoff value is chosen as $\Lambda = 2.1$ fm^{-1}.

In the $T = 0$ channel, the effect of the renormalization procedure on the short-range part of the tensor force is comparable to that of the central force, while in the $T = 1$ channel this effect is almost negligible. This is a quite remarkable feature. Let us discuss this feature in some detail by considering the Schrödinger equation for the deuteron. The deuteron has isospin $T = 0$, spin $S = 1$, orbital momentum $L = 0$ (S wave), and total angular momentum $J = 1$. There is a small admixture of D waves as well, leading to the following coupled differential equations for the deuteron:

$$\begin{aligned} &-\frac{\hbar^2}{M}\frac{d^2u(r)}{dr^2} + V_{\rm C}u(r) + \sqrt{8}V_{\rm T}w(r) = E_d u(r), \\ &-\frac{\hbar^2}{M}\frac{d^2w(r)}{dr^2} + \left(\frac{6\hbar^2}{Mr^2} + V_{\rm C} - 2V_{\rm T} - 3V_{\rm LS}\right)w(r) \\ &\qquad + \sqrt{8}V_{\rm T}u(r) = E_d w(r), \end{aligned} \tag{8}$$

where $u(r)$ and $w(r)$ are the radial wave functions of the S wave and the D wave, respectively. The potentials $V_{\rm C}$, $V_{\rm LS}$, and $V_{\rm T}$ are the central, spin-orbit, and tensor forces, respectively. Knowing the solution of Eq. (8), we can integrate out the D-wave degrees of freedom and obtain the following effective central force:

$$\begin{aligned} V_{\rm eff}(r;{}^3S_1) &= V_{\rm C}(r;{}^3S_1) + \Delta V_{\rm eff}(r;{}^3S_1), \\ \Delta V_{\rm eff}(r;{}^3S_1) &\equiv \sqrt{8}V_{\rm T}(r)\frac{w(r)}{u(r)}. \end{aligned} \tag{9}$$

The effective central force $\Delta V_{\rm eff}$ is comparable to $V_{\rm C}$ in strength and it makes the ${}^3S_1$ channel the most attractive one [17,18]. This effective central force makes the deuteron bound for the ${}^3S_1$ channel. We can regard this equation as a special case of Eq. (3). The effective central force comes from a second-order effect due to tensor force since both the initial and the final states have orbital angular momentum 0. As a consequence, the effective interaction for the $T = 0$ channel is enhanced by the renormalization procedure due to the short-range part of the tensor force. This is, however, not the case in the $T = 1$ channel. It reflects the property of the deuteron, which is the only bound two-nucleon system. A similar mechanism may also explain the strong cutoff dependence of the $V_{\rm low}k$ interaction seen in the $T = 0$ channel.

V. TENSOR FORCE IN EFFECTIVE INTERACTION FOR THE SHELL MODEL

We discuss here the tensor-force component in the effective interactions for the shell model, using the decomposition of Eq. (7). We have calculated effective interactions for the shell model $V_{\rm eff}^{\rm SM}$ using many-body perturbation theory by considering the $\hat{Q}$ box up to second and third order with folded diagrams included as well, starting from a renormalized $V_{\rm low}k$ interaction. The cutoff value used in the $V_{\rm low}k$ calculation is set to $\Lambda = 2.1$ fm^{-1} [15]. The model space (P space) is chosen to be the full sd shell or the full pf shell. In the construction of the $V_{\rm low}k$ interaction, we renormalize the strong short-range repulsion of the NN interaction, and in MBPT we include further effects of truncations of the model space. The $\hat{Q}$ box is calculated by considering valence-linked and connected diagrams with unperturbed single-particle energies of the harmonic oscillator. The oscillator energy $\hbar\omega$ is set to be 14 and 11 MeV for the sd-shell and the pf-shell effective interactions, respectively. Degenerate perturbation theory is employed in constructing the effective interactions.

Since the Q space is defined as the complement of the P space, intermediate states arising in each diagram should be taken up to infinitely high oscillator shells. In our case, using a low-momentum interaction $V_{\rm low}k$ with $\Lambda = 2.1$ fm^{-1}, full convergence of the monopole part of $V_{\rm eff}$ is obtained with approximately 8–10 $\hbar\omega$ excitations in each diagram that makes up the $\hat{Q}$ box.

Figure 4 shows the monopole part of the tensor force of $V_{\rm eff}^{\rm SM}$ defined for the sd shell or the pf shell. As a general trend, one can see again that the monopole part of the tensor force of $V_{\rm eff}^{\rm SM}$ fulfills our RP hypothesis to a good extent both in the sd shell and in the pf shell. Since the first-order $\hat{Q}$ box is just the $V_{\rm low}k$ interaction, the results mean that the monopole part of the tensor force is dominated by the first-order term in the $\hat{Q}$ box and the contributions from second- or higher-order terms are remarkably small. These results can be understood by considering the specific angular momentum structure of the tensor force, which is a scalar product of two rank 2 tensors in spin and coordinate spaces. In a perturbative correction to second or higher order, such a complicated structure is smeared out, and the resulting interaction consists mainly of a central force contribution. Therefore, as for the tensor-force component in the monopole interaction, it is the first-order contribution that is the dominant one.

To elucidate why higher-order terms in many-body perturbation theory are small, we consider as an example a contribution from second order in the interaction, by far the largest higher-order term.

The Hamiltonian causing the present second-order perturbation can be written as

$$H_1 = \sum_{p=0,1,2} w_p (U^{(p)} \times X^{(p)}), \tag{10}$$

where w_p represents an interaction strength and $U^{(p)}$ and $X^{(p)}$ are operators of rank p in spin space and coordinate space, respectively. A contribution from second order in perturbation theory to a state ϕ can then be written as

$$\eta(\phi) = -\sum_j \frac{\langle\phi|H_1|\psi_j\rangle\langle\psi_j|H_1|\phi\rangle}{\Delta E_j}, \tag{11}$$

where ψ_j defines an intermediate state with energy denominator ΔE_j. The summation is done over all intermediate states ψ_j. As far as ψ_j varies in this summation, within a fixed configuration with respect to harmonic-oscillator (HO) shells, ΔE_j remains constant due to the degeneracy of single-particle energies in a given HO shell. We mention that the usage of nondegenerate perturbation theory yields only small changes.

Such a configuration for a given HO shell is denoted by S. As ΔE_j is a constant within a fixed shell S, we label it as ΔE_S. Note that S corresponds to a part of the Q space, while ϕ is in the P space. The term $\eta(\phi)$ can then be decomposed

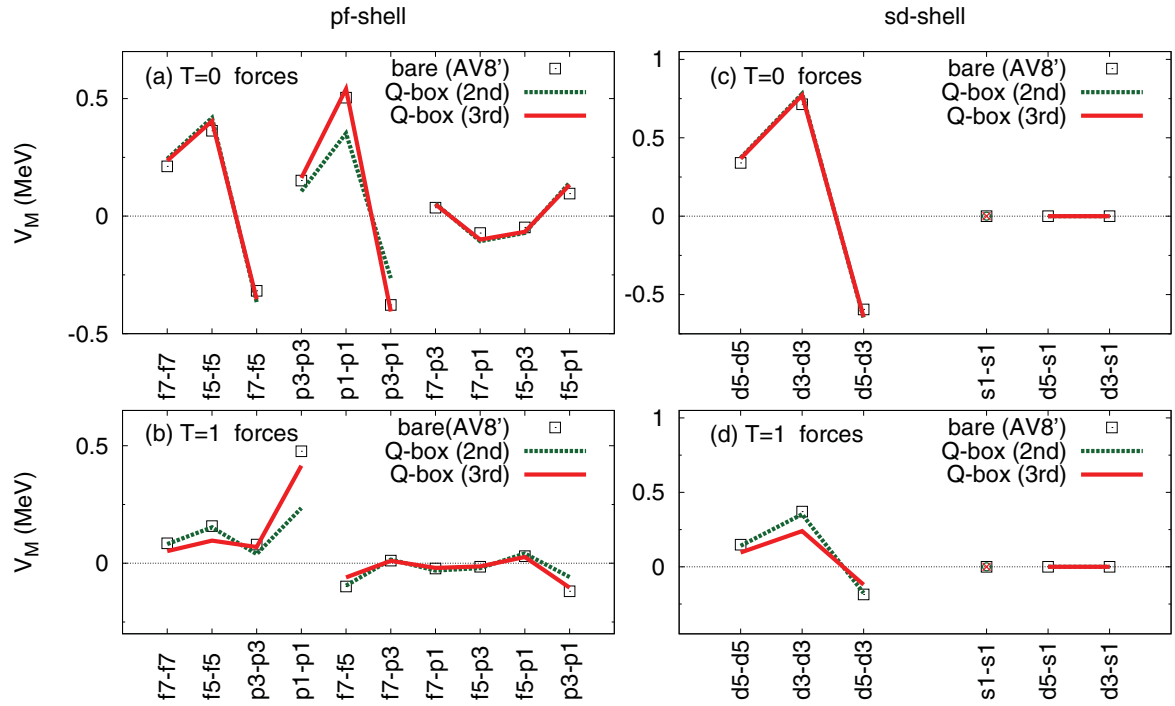

FIG. 4. (Color online) The tensor-force monopole component of the effective interaction for the shell model obtained by the $\hat{Q}$ box expansion to second and third order in the interaction, starting from $V_{\mathrm{low}k}(\Lambda = 2.1\ \mathrm{fm}^{-1})$. The tensor-force component is obtained using the decomposition of Eq. (7). (a) $T = 0$ forces in the pf shell, (b) $T = 1$ forces in the pf shell, (c) $T = 0$ forces in the sd shell, and (d) $T = 1$ forces in the sd shell.

into contributions from individual S's as

$$\eta(\phi) = -\sum_S \frac{\zeta(\phi, S)}{\Delta E_S}, \tag{12}$$

where

$$\zeta(\phi, S) = \sum_{j\in S} \langle\phi|H_1|\psi_j\rangle\langle\psi_j|H_1|\phi\rangle. \tag{13}$$

For a given S, all ψ_js are included, and the summation can be replaced by the closure relation as

$$\zeta(\phi, S) = \langle\phi|\{H_1 H_1\}_S|\phi\rangle, \tag{14}$$

where the braces $\{\ \}_S$ are introduced to indicate that the second H_1 changes ϕ to an S-configuration state in the Q space and the first H_1 moves it back to state ϕ in the P space. In other words, $H_1 H_1$ in this equation cannot be a simple product, but a certain contraction is needed, as we shall show soon.

By utilizing Eq. (10), we obtain

$$\begin{aligned}\{H_1 H_1\}_S &= \sum_{p_1,p_2} w_{p_1} w_{p_2} \{(U^{(p_1)} \times X^{(p_1)})(U^{(p_2)} \times X^{(p_2)})\}_S \\ &= \sum_{k=0,1,2} (2k+1)\left(\sum_{p_1,p_2} w_{p_1} w_{p_2} \begin{Bmatrix} p_1 & p_2 & k \\ p_1 & p_2 & k \\ 0 & 0 & 0 \end{Bmatrix} \{[[U^{(p_1)} \times U^{(p_2)}]^{(k)} \times [X^{(p_1)} \times X^{(p_2)}]^{(k)}]^{(0)}\}_S\right),\end{aligned} \tag{15}$$

where the terms in curly braces are $9j$ symbols and k implies the rank of the recoupling. The operator $\{[U^{(p_1)} \times U^{(p_2)}]^{(k)}\}_S$ acts in the P space as a rank-k two-body operator in spin space, while $\{[X^{(p_1)} \times X^{(p_2)}]^{(k)}\}_S$ acts as a rank-k two-body operator in coordinate space. Because the contraction due to the elimination of the Q space does not affect the angular momentum properties, the variable $k = 0, 1, 2$ represents induced central, spin-orbit, and tensor forces in the P space, respectively.

Since we are mainly interested in the tensor component, we focus on the case of $k = 2$, with the obvious restriction $p_1 + p_2 \geqslant 2$. Since the above $9j$ symbols are proportional to $1/\sqrt{(2p_1+1)(2p_2+1)}$, it is easy to convince oneself that the central-force component receives the largest contribution from the $9j$ symbol. Furthermore, for our analyses it is important to keep in mind that the expectation value of the central component is the largest in absolute value, the tensor component is the second largest, and the spin-orbit term gives rise to the smallest contribution to the renormalized $V_{\mathrm{low}k}$ interaction.

From these considerations, for $k = 2$ the largest contribution comes from the combination $p_1 = 0$, $p_2 = 2$ or $p_1 = 2$, $p_2 = 0$ in Eq. (10), that is, either a central-tensor or a tensor-central combination. Let us now discuss this case. We assume without loss of generality that the tensor component of H_1 acts on the ket state of the matrix element being considered. While the central component of H_1 acts afterward on this state, we can also consider that this central force acts to the left on the bra state. We then take the overlap between these two states by considering one by the tensor on the ket side and the other by the central on the bra side. These two states are sum-rule states for the two forces within the S-configuration space. As the central force and the tensor force are very different in nature, such sum-rule states are very different from each other in general, leading to a very small overlap. This is the main reason why the combination of the central force and the tensor force produces small contributions.

This argument does not hold for the case where the tensor component of H_1 acts twice in the term to second order in perturbation theory. However, due to the angular momentum coupling, the product of two tensor forces [$p_1 = p_2 = 2$ in Eq. (10)] yields small contributions to the $k = 2$ terms of Eq. (10). For higher orders, other tensor-force components may show up, but there is no mechanism to enhance their contributions.

The small contribution of the tensor force in MBPT can be viewed to be reasonable also under the following intuitive picture: after multiple actions of the forces, the spin dependence is smeared out, and only the distance between two interacting nucleons becomes the primary factor to the whole processes. This results in the dominance of the induced effective interaction by the central components and yields only a minor change in the tensor component.

It is instructive to study in more detail the contributions to second order in perturbation theory. To do so, we single out the by far largest second-order term, namely, the so-called core-polarization term [Fig. 1(c)]. For the core-polarization diagram we can show that the contribution to the tensor force vanishes by simple angular momentum algebra arguments. The contribution to a specific core-polarization matrix element can then be written as

$$\begin{aligned}\langle am_a bm_b|V_T^{\mathrm{cp-eff}}|cm_c dm_d\rangle &= \sum_{p,m_p,h,m_h} \langle am_a pm_p|V_C|cm_c hm_h\rangle\langle hm_h bm_b|V_T|pm_p dm_d\rangle/\Delta E \\ &= \sum_{n_p,l_p,n_h,l_h}\left(\sum_{j_p,m_p,j_h,m_h}\langle am_a pm_p|V_C|cm_c hm_h\rangle\langle hm_h bm_b|V_T|pm_p dm_d\rangle\right)\Big/\Delta E_S \\ &= \sum_{n_p,l_p,n_h,l_h}\left(\sum_{m_{lp},m_{sp},m_{lh},m_{sh}}\langle am_a n_p l_p m_{lp} m_{sp}|V_C|cm_c n_h l_h m_{lh} m_{sh}\rangle\right. \\ &\quad \left.\times\langle n_h l_h m_{lh} m_{sh} bm_b|V_T|n_p l_p m_{lp} m_{sp} dm_d\rangle\right)\Big/\Delta E_S, \end{aligned} \tag{16}$$

where $V_T^{\mathrm{cp-eff}}$ is the induced tensor force and V_T and V_C are the tensor-force and central-force components from H_1, respectively. With a harmonic oscillator basis, the term ΔE_S represents an energy denominator that is constant for a given set of quantum numbers n_p, n_h, l_p, and l_h, as discussed above. Here $a = (n_a, l_a, j_a)$, and m_a denotes the magnetic substate of l_a. Note that the two-body states are not antisymmetrized. The states p and h represent particle and hole states, respectively. In the third line of Eq. (16), only particle and hole states are transformed to the ls coupling scheme. Note that the intermediate states are summed up to fulfill spin saturation within each HO major shell.

We can divide the contribution into two different types according to the spin dependence of the central force. One comes from the terms whose central force part V_C includes $\sigma \cdot \sigma$ (type I) and the other does not (type II). With our summation tailored to a spin-saturated core or an excluded Q space with all spin-orbit partners, we can prove that type II contributions always vanish because the first factor is diagonal with respect to spin, that is, $m_{sp} = m_{sh}$, and the second factor is zero when we sum over spin-saturated contributions. Therefore, only a spin-dependent central force results in nonvanishing contributions to the tensor force for higher-order terms in $V_{\mathrm{eff}}^{\mathrm{SM}}$. Finally, the contribution to the tensor force from the spin-dependent central force is quite small because the spin-dependent central force is generally by far smaller than the spin-independent central force in modern realistic NN potentials.

In conclusion, medium effects produce minor contributions to the tensor-force component, resulting in a tensor-force component that is dominated by the bare NN interaction. Our hypothesis about renormalization persistency is fulfilled to a good extent by the tensor force.

Finally, although our analyses have been performed within one major shell only, one should note that this persistency of the tensor-force component via a MBPT renormalization should also hold for model spaces that span several shells.

VI. TWO-BODY MATRIX ELEMENTS OF THE TENSOR FORCE

In this section we study further renormalization properties of the tensor force by including higher multipole components.

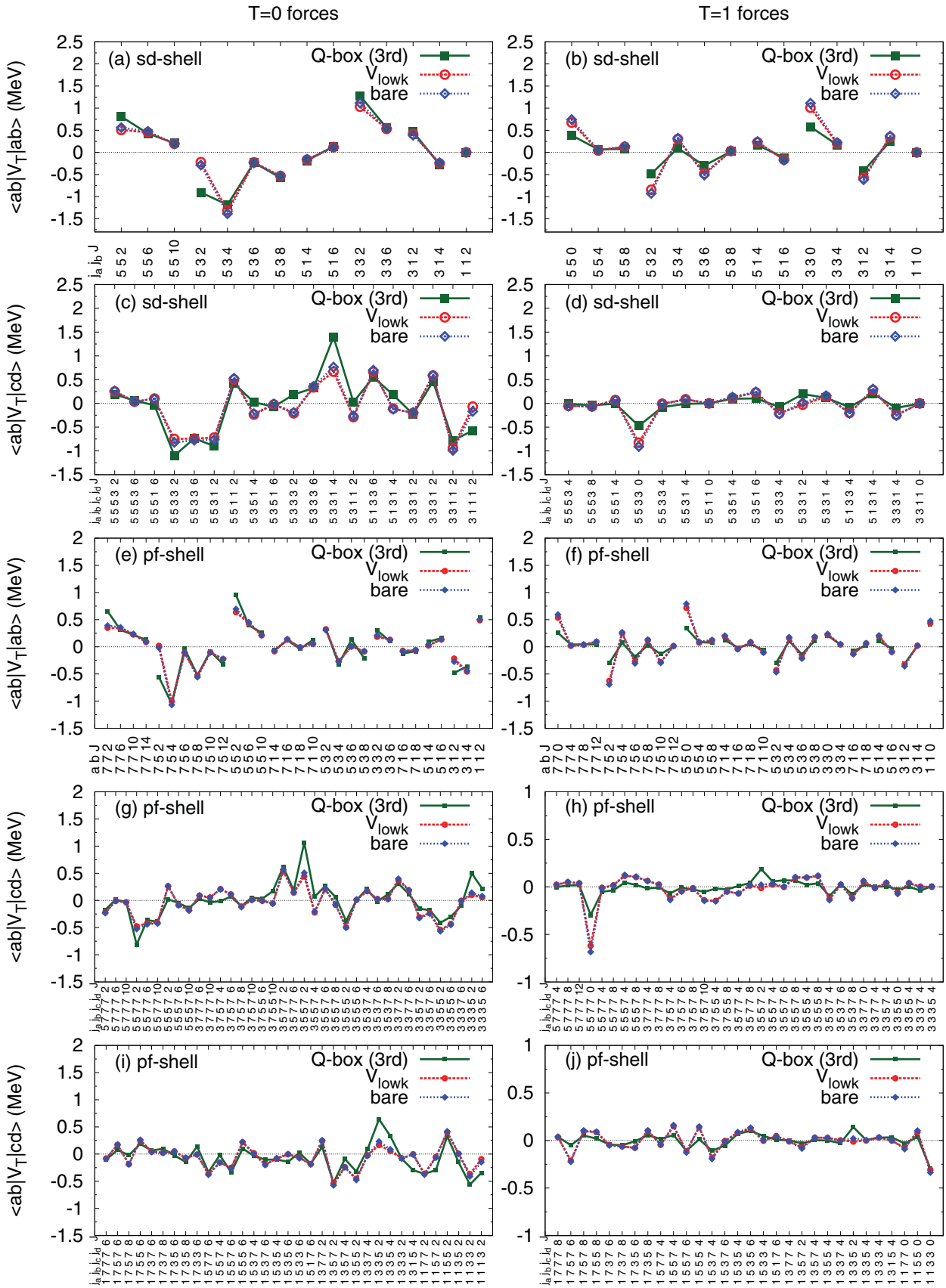

FIG. 5. (Color online) Diagonal and nondiagonal matrix elements of the tensor-force component from effective interactions using the AV8' potential.

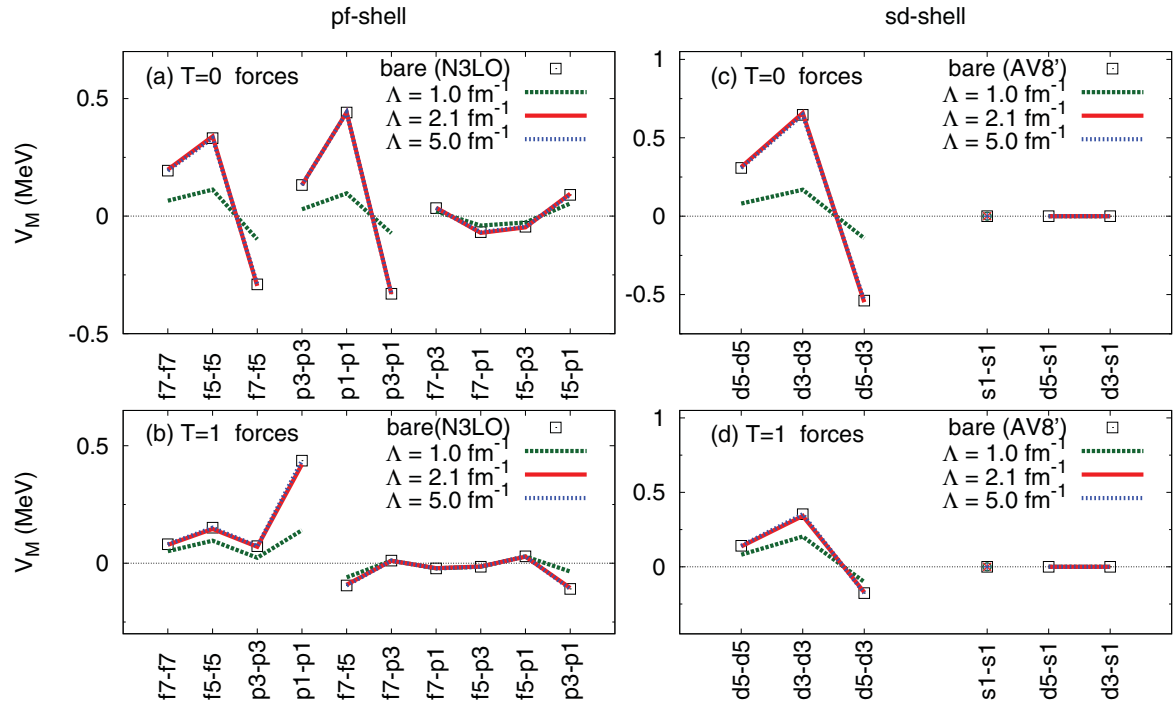

FIG. 6. (Color online) Tensor-force monopole of $V_{\mathrm{low}k}$ starting from the χN^{3}LO interaction with the same notation as in Fig. 2.

Figure 5 shows the diagonal and nondiagonal matrix elements of the bare tensor force from the AV8' potential, the renormalized $V_{\mathrm{low}k}$ interaction ($\Lambda = 2.1$ fm^{-1}), and $V_{\mathrm{eff}}^{\mathrm{SM}}$ obtained by the $\hat{Q}$-box expansion up to the third order with folded diagrams to infinite order starting from AV8' interaction. This is similar to what was done in Figs. 2 and 4. Figures 5(a) to 5(d) show the sd-shell matrix elements. The diagonal matrix elements are shown in Figs. 5(a) and 5(b), while the nondiagonal elements are shown in Figs. 5(c) and 5(d). Note that the diagonal matrix elements $\langle j_a j_b | V | j_a j_b \rangle_{JT}$ are specified by the quantum numbers j_a, j_b and twice the total angular momentum J and total isospin T. The nondiagonal matrix elements $\langle j_a j_b | V | j_c j_d \rangle_{JT}$ are specified by j_a, j_b, j_c, j_d, J, and T. The corresponding numbers for the pf shell are shown in Figs. 5(e)

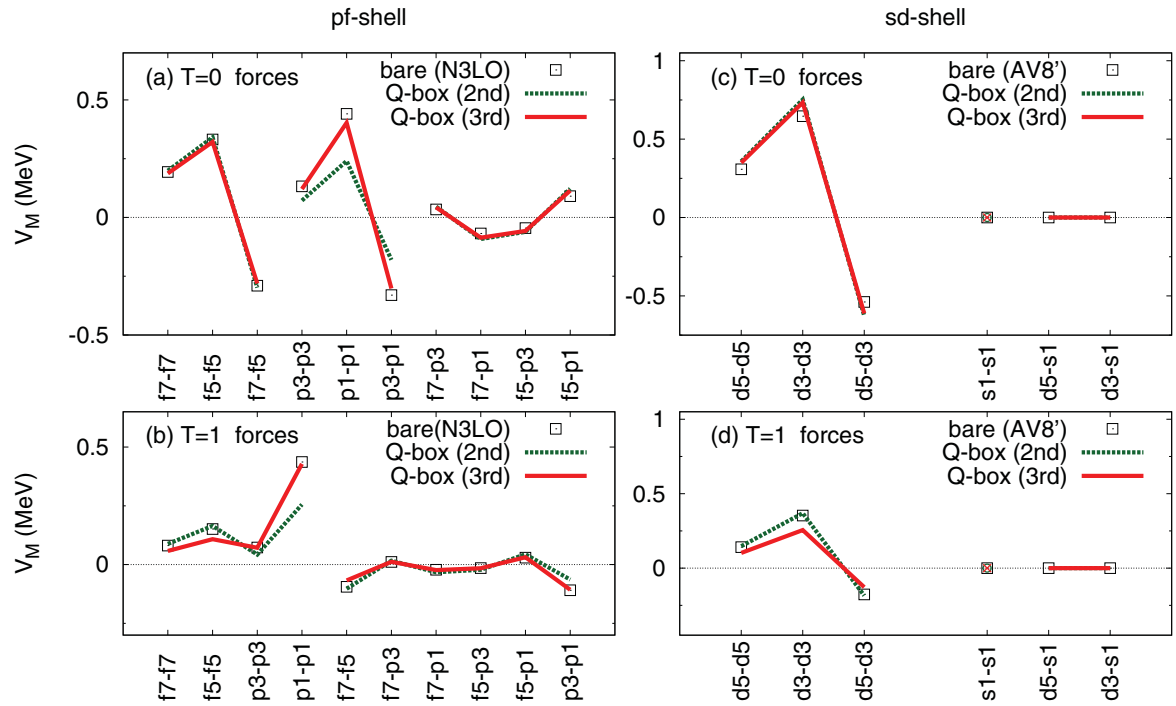

FIG. 7. (Color online) Tensor-force monopole of $V_{\mathrm{eff}}^{\mathrm{SM}}$ starting from the χN^{3}LO with the same notation as in Fig. 4.

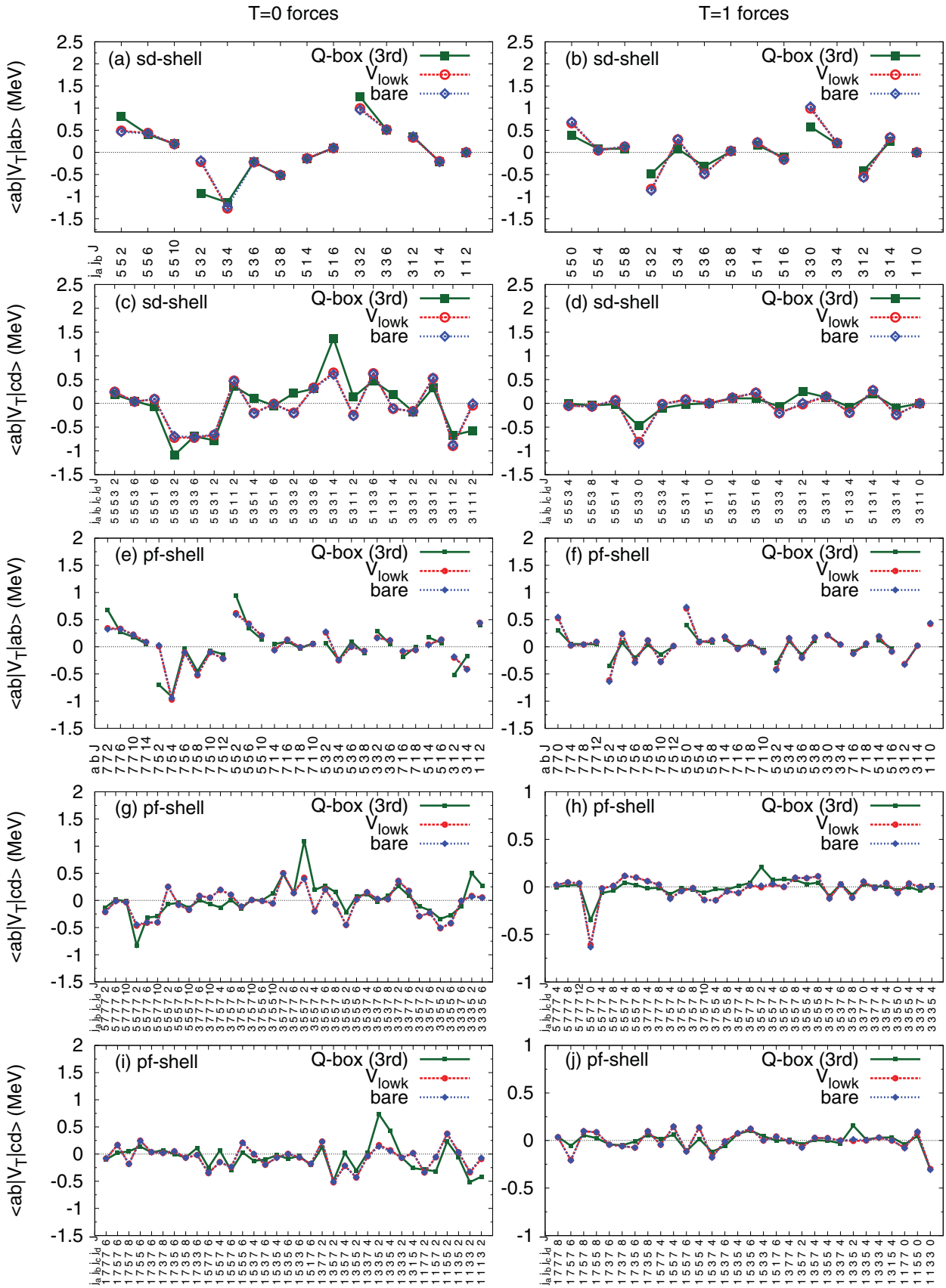

FIG. 8. (Color online) Diagonal and nondiagonal matrix elements of the tensor-force component from effective interactions using the χN^{3}LO interaction. The labeling is the same as in Fig. 5.

through 5(j). In both the sd shell and the pf shell, the patterns are the same for all approaches to the effective interactions and thus the RP is approximately fulfilled. In particular, for the $V_{\mathrm{low}k}$ renormalization procedure, we can hardly see any difference between the bare tensor force and the tensor force in the effective interaction $V_{\mathrm{low}k}$. For the diagonal matrix elements, we can see small differences between the final $\hat{Q}$ box and the bare tensor force; however, it does not contradict the results with respect to the monopole component discussed above, mainly because only matrix elements with small values of the total angular momentum display sizable differences. Since the monopole terms are weighted by $2J + 1$, matrix elements with larger values of the total angular momentum J carry a much larger weight in Eq. (1). In nondiagonal matrix elements, we see somewhat larger differences. Their role in shell-model calculations needs to be investigated further. A spin-tensor analysis along these lines was made recently by Smirnova *et al*. [19].

VII. ANALYSIS OF OTHER INTERACTION MODELS

In the previous sections, we calculated effective interactions starting from the AV8' interaction, using a renormalized interaction and many-body perturbation theory. We found that the RP of the tensor force holds for all these renormalization procedures. An obvious question is whether or not the RP holds for other interaction models as well. In this section we address this issue as well.

We employ here another frequently used realistic interaction, χN^{3}LO, as an example [11]. The χN^{3}LO interaction has a relatively smaller coupling between low-momentum and high-momentum modes compared with the AV8' potential. In Fig. 6 we show the monopole part of the tensor force of the χN^{3}LO bare potential and $V_{\mathrm{low}k}$ with several cutoff parameters Λ(1.0, 2.1, and 5.0 fm^{-1}). These results should be compared with the corresponding ones obtained with the AV8' interaction shown in Fig. 2. Figure 7 shows the tensor-force monopole of $V_{\mathrm{eff}}^{\mathrm{SM}}$, corresponding to Fig. 4 for the AV8' interaction, starting from the χN^{3}LO interaction. Finally, Fig. 8 shows the multipole components of effective interactions, corresponding to Fig. 5 for the AV8' interaction.

In all the figures, we can conclude that all the features we discussed for the AV8' interaction pertain to the χN^{3}LO interaction model as well.

VIII. CONCLUSION

In this work we have presented a detailed analysis of various contributions to the nuclear tensor force as function of different renormalization procedures, starting with state-of-the-art nucleon-nucleon (NN) interactions and ending up with effective interactions for the nuclear shell model. The monopole part of the tensor force is weakly or barely affected by various renormalization procedures, which in our case are represented by a renormalization of the bare interaction and many-body perturbation theory in order to obtain an effective shell-model interaction. This has led us to introduce the concept of renormalization persistency in the study of effective interactions. We studied the RP of both renormalization procedures and showed via numerical studies, their intuitive general explanations, and a detailed algebraic analysis of core-polarization terms in perturbation theory that this is a very robust process. We have also shown that the RP holds for two-body matrix elements including higher-multipole components of the tensor force, although the deviation increases somewhat if multipole components are included in the comparison. We conclude that the two renormalization steps (one for short-range correlation and the other for in-medium effects) do not affect much either the monopole or the multipole components of the tensor force, apart from slight differences between them. Results obtained with two different interactions (AV8' and χN^{3}LO) led us to the same conclusion, suggesting that the RP of the tensor force for low-momentum states is a robust feature. This applies also to interaction models other than those studied here.

The short-range part of the tensor force enters the renormalization of the central force, in particular in the $T = 0$ channel, producing on average an increased attraction. Since the modification of the tensor force appears to be small, the central force carries most of the renormalization effects beyond first order in perturbation theory.

Because the RP of the tensor force in effective interactions is a robust feature, it may give a simple and concrete starting point for examining and constructing effective interactions, especially phenomenological ones [4]. In particular, since the tensor force plays a significant role in the shell evolution for nuclear systems with either large neutron/proton or proton/neutron ratios, one can extract simple physics messages from complicated many-body systems.

ACKNOWLEDGMENTS

We are very grateful to Professor R. Okamoto and Professor H. Feldmeier for valuable discussions. This work is supported in part by Grant-in-Aid for Scientific Research (A) No. 20244022 and also by Grant-in-Aid by the JSPS (Grant No. 228635) and by the JSPS Core to Core program "International Research Network for Exotic Femto Systems" (EFES).

[1] R. B. Wiringa, V. G. J. Stoks, and R. Schiavilla, Phys. Rev. C **51**, 38 (1995).
[2] R. B. Wiringa and S. C. Pieper, Phys. Rev. Lett. **89**, 182501 (2002).
[3] T. Otsuka, T. Suzuki, R. Fujimoto, H. Grawe, and Y. Akaishi, Phys. Rev. Lett. **95**, 232502 (2005).
[4] T. Otsuka, T. Suzuki, M. Honma, Y. Utsuno, N. Tsunoda, K. Tsukiyama, and M. Hjorth-Jensen, Phys. Rev. Lett. **104**, 012501 (2010).
[5] R. Bansal and J. French, Phys. Lett. **11**, 145 (1964).
[6] A. Poves and A. Zuker, Phys. Rep. **70**, 235 (1981).

[7] S. Bogner, T. T. S. Kuo, L. Coraggio, A. Covello, and N. Itaco, Phys. Rev. C **65**, 051301 (2002).
[8] S. K. Bogner, T. T. S. Kuo, and A. Schwenk, Phys. Rep. **386**, 1 (2003).
[9] T. Kuo and E. Osnes, *Folded-Diagram Theory of the Effective Interaction in Nuclei, Atoms and Molecules*, Lecture Notes in Physics, Vol. 364 (Springer, Berlin, 1990).
[10] M. Hjorth-Jensen, T. T. S. Kuo, and E. Osnes, Phys. Rep. **261**, 125 (1995).
[11] E. Epelbaum, H.-W. Hammer, and U.-G. Meißner, Rev. Mod. Phys. **81**, 1773 (2009).
[12] M. W. Kirson, Phys. Lett. B **47**, 110 (1973).
[13] E. Osnes and D. Strottman, Phys. Rev. C **45**, 662 (1992).
[14] B. A. Brown, W. A. Richter, R. E. Julies, and B. H. Wildenthal, Ann. Phys. (NY) **182**, 191 (1988).
[15] A. Nogga, S. K. Bogner, and A. Schwenk, Phys. Rev. C **70**, 061002 (2004).
[16] S. K. Bogner, A. Schwenk, T. T. S. Kuo, and G. E. Brown, arXiv:nucl-th/0111042v1.
[17] A. Umeya and K. Muto, Phys. Rev. C **74**, 034330 (2006).
[18] R. Tamagaki and W. Watari, Prog. Theor. Phys. Suppl. **39**, 23 (1967).
[19] N. A. Smirnova, B. Bally, K. Heyde, F. Nowacki, and K. Sieja, Phys. Lett. B **686**, 109 (2010).